

Molecular dynamics of poly(L-lactide) biopolymer studied by wide-line solid-state ^1H and ^2H NMR spectroscopy

Farhod Nozirov^a, Alovidin Nazirov^b, Stefan Jurga^b, Riqiang Fu^{a,*}

^aCenter for Interdisciplinary Magnetic Resonance, National High Magnetic Field Laboratory, 1800 East Paul Dirac Drive, Tallahassee, FL 32310, USA

^bDepartment of Macromolecular Physics, Adam Mickiewicz University, Umultowska 85, 61-614 Poznań, Poland

Received 28 April 2005; received in revised form 31 August 2005

Available online 3 October 2005

Abstract

The molecular dynamics of poly(L-lactide) (PLLA) biopolymer was characterized through analyses of ^1H and ^2H NMR line-shapes and spin-lattice relaxation times at different temperatures. At low temperatures (e.g. 90 K), the methyl group rotation is dominant leading to a significant reduction in the proton second moment. Fast methyl group reorientation occurs at ca. 130 K. In addition to the fast methyl group rotation, hydroxyl groups start to reorient as the temperature increases further, eventually leading to the breakdown of the segments of the biopolymer chains above its glass transition temperature T_g of 323 K. The analyses of the ^2H NMR line-shapes indicate that both the methyl and hydroxyl reorientations can be described by the so-called cone model, in which the former has three equilibrium positions with $\theta_{\text{C-D}} = 70.5^\circ$ and $\phi = 120^\circ$ while the latter one exhibits two equilibrium positions with $\theta_{\text{O-D}} = 78^\circ$ and $\phi = 180^\circ$.

© 2005 Elsevier Inc. All rights reserved.

Keywords: Poly(L-lactide) (PLLA); Biopolymer; Molecular dynamics; Spin-lattice relaxation; Solid state NMR

1. Introduction

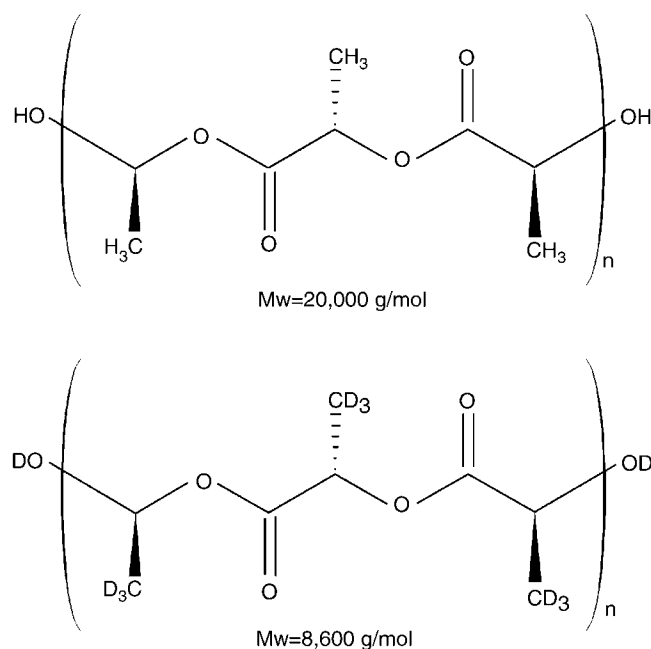
Aliphatic polyesters such as polylactide (PLA), polyhydroxybutyrate (PHB) polyglycolide (PGA), polycaprolactone, and their copolymers have recently received considerable attention because of their widespread applications in nutrition and medicine [1–10], for example, plastic bags and bottles used in the food industry, drug release capsules, surgical sutures, gauzes, bandages, bone plates, and so on. High molecular mass PLA shows mechanical and barrier behavior comparable to synthetic polymers such as polystyrene (PS) and polyethylene terephthalate (PET) [11]. X-ray analysis [12,13] indicated that PLA crystallizes in the orthorhombic lattice unit cell with $a = 1.07$, $b = 0.645$, and c (chain axis) = 2.78–1.05 nm. It was shown that PLA forms the 10_3 α -helical conformation [14], while the Monte Carlo simulation studies indicated a hexagonal molecular packing with the existence of shifting

chain axis and setting angles [15]. However, the molecular dynamics of such materials has not been well understood, even though some materials such as PHB [16–18] and glycolide/caprolactone copolymer [19] have been studied. Here, comprehensive solid state nuclear magnetic resonance (NMR) studies are performed in order to understand the molecular dynamics of poly(L-lactide) (PLLA) biopolymer in solid state. Scheme 1 shows the schematics of the PLLA structure and the deuteron positions in the polymeric repeat unit.

It has been shown that PLLA micro-spheres strongly depend on the degree of crystallinity, which can be controlled by its molecular weight [20]. Different PLLA crystal formations, such as α and β , were obtained, depending on the spinning and drawing conditions [21]. The ^{13}C NMR spectra of highly crystalline PLLA showed at least five distinct resonances for the carbonyl and methine functional groups, signifying crystallographically inequivalent sites in the crystalline domains [22,23]. It was further concluded through the carbonyl resonances that there exist conformational changes between the monomer units in the PLLA polymer matrix.

*Corresponding author. Fax: +850 644 1366.

E-mail addresses: nozirov@magnet.fsu.edu (F. Nozirov), rfu@magnet.fsu.edu (R. Fu).



Scheme 1.

NMR spectroscopy is known to be uniquely suitable for the study of molecular dynamics in solids [24,25]. For instance, proton second moments are sensitively related to motional states in solids [26]. The ^1H spin-lattice relaxation is governed by proton dipolar interactions modulated by molecular motions. On the other hand, ^2H NMR is very sensitive to local dynamics, thus providing detailed information on morphology, molecular motion, and reorientation in solids [27]. In this work, we use various wide-line solid-state ^1H and ^2H NMR techniques, in combination with the differential scanning calorimetry (DSC), to study the molecular dynamics of the PLLA biopolymer.

2. Experimental

2.1. Samples

A sample of PLLA with a molecular weight of 20,000 g/mol was purchased from Aldrich. A PLLA sample selectively deuterated at the methyl and hydroxyl groups was kindly provided by Dr. Jean-Louis Morgat at the University of Montpellier, France. The degree of the deuteration was estimated at ca. 95% using Fourier-transform infrared (FTIR) and ^2H solid-state NMR spectroscopy. Its molecular weight $M_w = 8600$ g/mol was determined using the Gel permeation chromatography (GPC) technique.

2.2. Differential scanning calorimetry (DSC)

For DSC thermograms, the PLLA (5 mg) and the selectively deuterated PLLA (5 mg) samples were contained

in sealed aluminum pans and placed in a Netzsch DSC-204 differential scanning calorimetry. The temperature was scanned between 100 and 523 K with a heating rate of 10 K/min. The samples were first heated from 100 to 523 K and held at that temperature for 1 min. After cooling back down to 100 K, the samples were again heated to 523 K at the rate of 10 K/min.

2.3. NMR spectroscopy

Samples for NMR were sealed in glass ampoules after they were degassed by evacuation for 48 h at room temperature to remove paramagnetic oxygen and the trace of water in order to eliminate the effects of the paramagnetic impurities on the longitudinal relaxation times [28]. The derivatives of ^1H NMR absorption spectra were registered with the continuous-wave method on a lab-made apparatus operating at 25 MHz. ^1H spin-lattice relaxation times at 200 MHz were measured on a Bruker CXP spectrometer using a saturation recovery sequence of sixteen $\pi/2 - \tau - \pi/2$ pulses. The ^2H NMR experiments were performed on a Bruker CXP NMR spectrometer operating at 30.7 MHz. The line-shapes were recorded using the quadrupolar echo sequence $(\pi/2)_x - \tau_Q - (\pi/2)_y - \tau_Q$ and the spin-lattice relaxation times were measured using the inversion-recovery pulse sequence $\pi - \tau - (\pi/2)_x - \tau_Q - (\pi/2)_y - \tau_Q$ [29], where the $\pi/2$ pulse length was 3 μs and a total of 15 different τ values was used. The echo time τ_Q of 15 μs was used in these experiments. The sample temperatures were controlled by a gas flow cryostat and monitored by the calibrated Pt resistance thermometer with an accuracy of 0.5 K.

3. Results

Fig. 1 shows the DSC thermograms of both the PLLA and the selectively deuterated PLLA samples in the temperature range of 100–523 K. As indicated in Fig. 1, the glass transition temperature, T_g was 323 K for the PLLA sample. While for the ^2H -PLLA, a sharp phase transition temperature, T_g was observed at 330 K during the first heating process. It is believed that this transition is the pseudo-first order [30] phase transition because the re-heating process shifts the glass transition temperature to 320 K, as seen in Fig. 1. The endothermic peaks at 448 K indicate the melting temperature, T_m of the crystalline phase of the PLLA. The peak at 378 K is attributed to the supercooling phase of PLLA [20]. For ^1H -PLLA, the DSC thermogram shows a relatively broad melting peak due to the coexistence of crystalline and amorphous phases in the biopolymer matrix. Crystallization of the ordered crystalline form took place at 370 K. The DSC analysis indicated that this ^1H -PLLA sample ($M_w = 20,000$ g/mol) has a degree of crystallinity $\alpha = 43.7\%$, which was calculated based on the formula $\alpha(\%) = 100 \times \Delta H_m / \Delta H$, [31] where ΔH_m is the enthalpy of the peak and ΔH denotes the enthalpy of melting of a pure crystalline sample [32]. In contrast, for the ^2H -PLLA sample, the matrix is made with

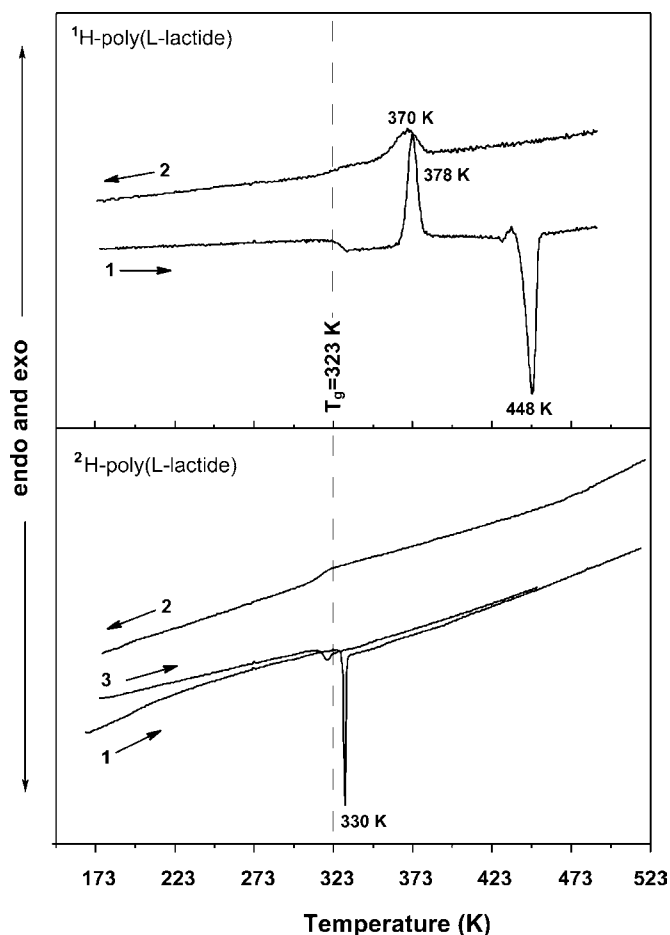


Fig. 1. DSC thermograms of proton and deuterated poly(L-lactide). 1-heating, 2-cooling, 3-reheating. The dashed line indicates the glass phase transition temperature, T_g .

the rigid amorphous phase, which is thermodynamically stable under the condition of an exchange reaction of ^1H to ^2H [33–35].

Fig. 2 shows the second moment M_2 of the ^1H NMR lines of PLLA as a function of temperature. At very low temperature (e.g. 90 K), the measured M_2 value is ca. 0.11 mT^2 . The M_2 value is decreased to 0.08 mT^2 as the temperature increases to 130 K but remains almost constant in the temperature range of 130–325 K. The M_2 value decreases gradually with a further increase in temperature and eventually reaches a second plateau of 0.031 mT^2 at 380 K.

Fig. 3 shows the recovery of ^1H magnetization from the PLLA sample at different temperatures. A bi-exponential recovery was found for all measurements below T_g as indicated in Fig. 3, implying that there exist two proton spin-lattice relaxation times T_1^{H} in the biopolymer. The bi-exponential fittings from the measurements at 150, 255, and 275 K yielded T_1 values of 1.0 and 0.5, 1.67 and 0.5, and 2.5 and 0.70 s, respectively. Generally, a single-exponential pattern of the spin-lattice relaxation is expected due to sufficient spin diffusion in strongly

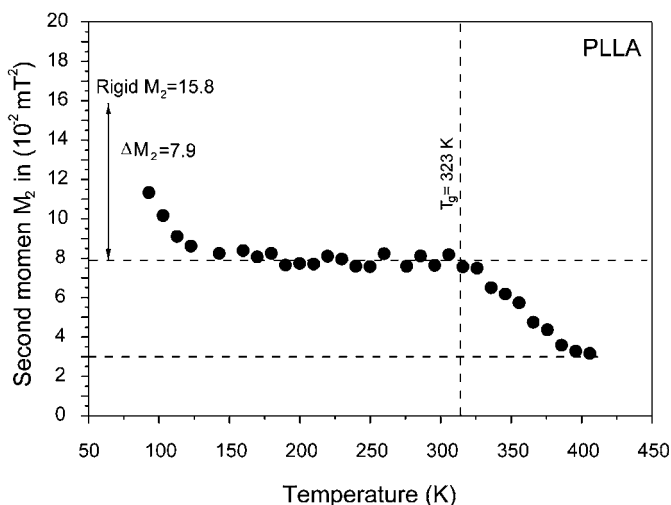


Fig. 2. Second moment of the ^1H NMR line of poly(L-lactide) versus temperature. The glass phase transition temperature, T_g is indicated by the vertical dashed line.

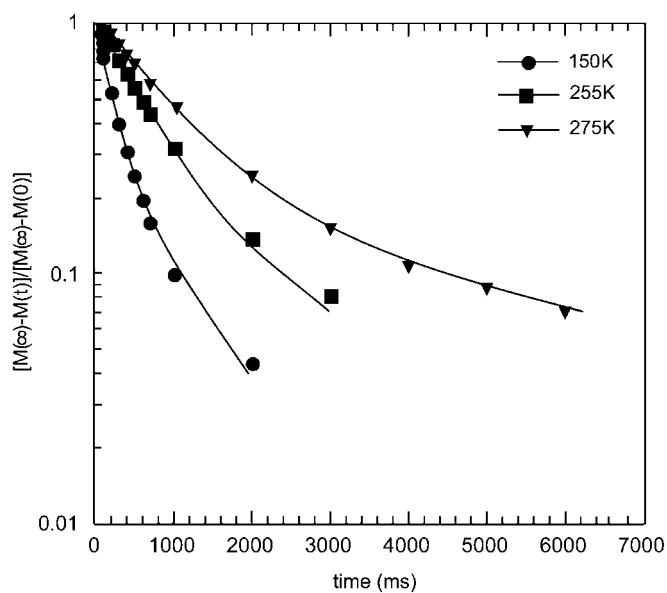


Fig. 3. Semilogarithmic plot of normalized integral ^1H signal intensities from the PLLA sample ($M_w = 20,000\text{ g/mol}$) as a function of recovery time. All of the experimental data were fitted using two exponential components as indicated by the solid lines. The two ^1H spin-lattice relaxation times (T_1) obtained from the measurements at 150, 255, and 275 K were 1.0 and 0.5, 1.67 and 0.5, and 2.5 and 0.70 s, respectively.

dipolar-coupled proton systems. However, in some cases where the proton coupling systems consist of two distinct spatially well-separated regions and the spins in the two regions can not communicate effectively through proton spin diffusion due to their different motional dynamics, two exponential spin-lattice relaxations were observed [36]. The bi-exponential fittings also indicated the composition of the two relaxation components, which in turn reveals the fractions of the two phases in the biopolymer. Fig. 4 shows the plot of the fractions of the two relaxation components

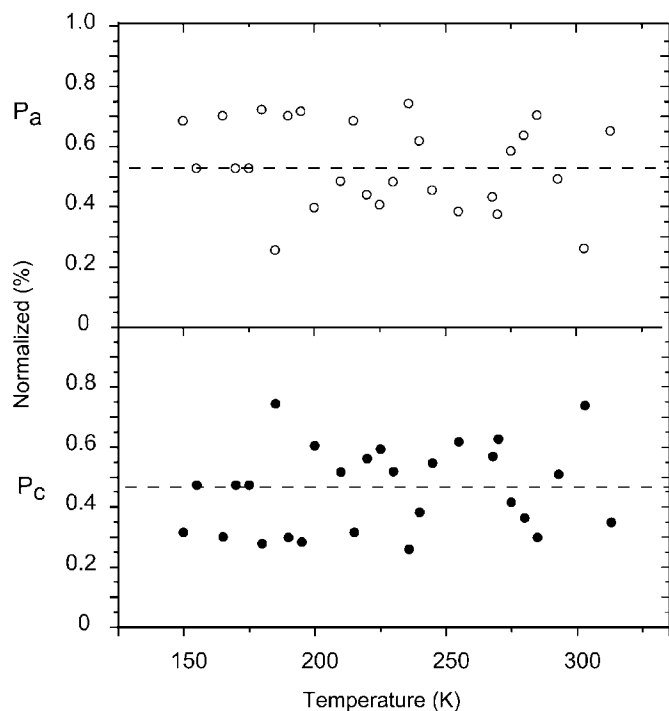


Fig. 4. Normalized weighting factors p_a and p_c of the two relaxation components obtained from the bi-exponential fittings of the ^1H relaxation measurements as a function of temperature. The weighting factors p_a and p_c correspond to the probability of the amorphous and crystalline phases coexisting in PLLA ($M_w = 20,000$ g/mol). The averages of the factors over the temperature range are indicated by the dashed lines, in good agreement with the degree of the crystallinity determined by the DSC analysis.

obtained from the relaxation measurements at different temperatures. Clearly, the average fraction is 54% and 46%, which is in good agreement with our DSC analysis indicating about 43.7% crystallinity in this ^1H -PLLA sample. Therefore, we may reasonably assume that the two relaxation components represent the amorphous and crystalline phases coexisting in the biopolymer matrix. The protons of the amorphous phase with a fraction p_a of 54% have a relatively short relaxation time while the protons of the crystalline phase with a fraction p_c of 46% exhibit a relatively long T_1 . At temperatures above T_g , a nearly single-exponential recovery was observed implying that the amorphous and crystalline phases are not distinguishable above T_g . In contrast, the recovery of ^2H magnetization from the selectively deuterated PLLA sample ($M_w = 8600$ g/mol) was found to be a single exponential, owing to the dominant ordered rigid amorphous phase.

Fig. 5 shows the ^1H and ^2H relaxation rates ($1/T_1$) in the Arrhenius representation (i.e. $1/T_1$ vs. $\beta = 1000/T$) for the PLLA and the deuterated PLLA samples. The two ^1H spin-lattice relaxation times shown in the plot were obtained via the bi-exponential fittings from the proton relaxation measurements, as shown in Fig. 3. Again, the two T_1 components represent two different phases (i.e. the

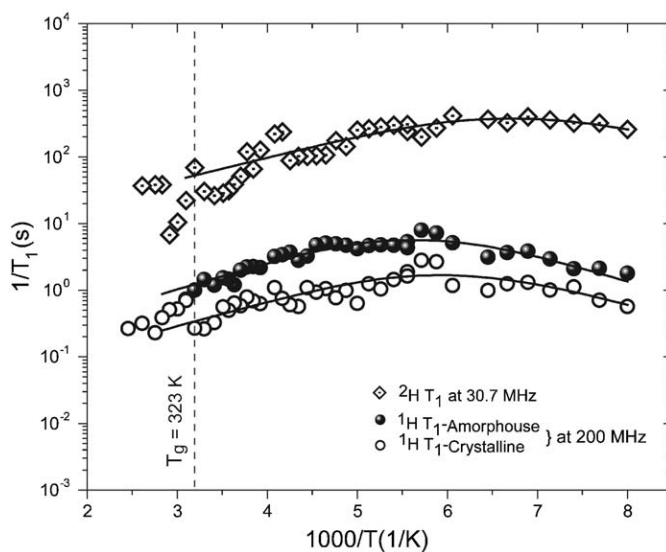


Fig. 5. Arrhenius plot of ^1H and ^2H relaxation rates ($1/T_1$) for the PLLA and the selectively deuterated PLLA samples. The ^1H experimental data were fitted by using Eqs. (3)–(5), while the ^2H experimental data were fitted by using Eqs. (5), (7), and (9), as indicated by the solid lines. The vertical line indicates the glass phase transition temperature, T_g .

amorphous and crystalline phases) in the biopolymer. The former exhibits a T_1 minimum of 0.2 s at 161 K (i.e. $\beta = 6.2$ K $^{-1}$) while the latter has a T_1 minimum of 0.5 s at 175 K (i.e. $\beta = 5.7$ K $^{-1}$). In contrast, for the selectively deuterated PLLA ($M_w = 8600$ g/mol), the ^2H spin lattice relaxation times at 30.7 MHz showed a T_1 minimum of 3.0 ms at 160 K (i.e. $\beta = 6.25$ K $^{-1}$). The vertical line indicates the temperature at which the glass transition takes place.

Fig. 6 shows the ^2H quadrupolar echoed NMR spectra of the selectively deuterated PLLA sample ($M_w = 8600$ g/mol) as a function of temperature in the range of 140–353 K. At 140 K, a well-defined Pake-doublet with a quadrupolar splitting of 37 kHz was clearly observed. The line-shape of this doublet does not change as the temperature goes up to 323 K, as shown in Fig. 6. It can be seen from Fig. 6 that another broad Pake-doublet with a quadrupolar splitting of 116 kHz became visible at 200 K. Such a broad doublet, without changing its line-shape, gains in intensity when the temperature is increased up to 323 K.

4. Discussion

4.1. Second moment M_2 of ^1H NMR lines

For a better understanding of the molecular dynamic processes taking place in the PLLA biopolymer, we used the Goc program [37] to calculate values of the ^1H second moment induced by the motional states using the bond distances of the atomic coordinates of the lactide. To facilitate the calculations, the rigid lattice value was broken up into intra- and intermolecular contributions. The intramolecular contribution M_2^{intra} , arising from interactions

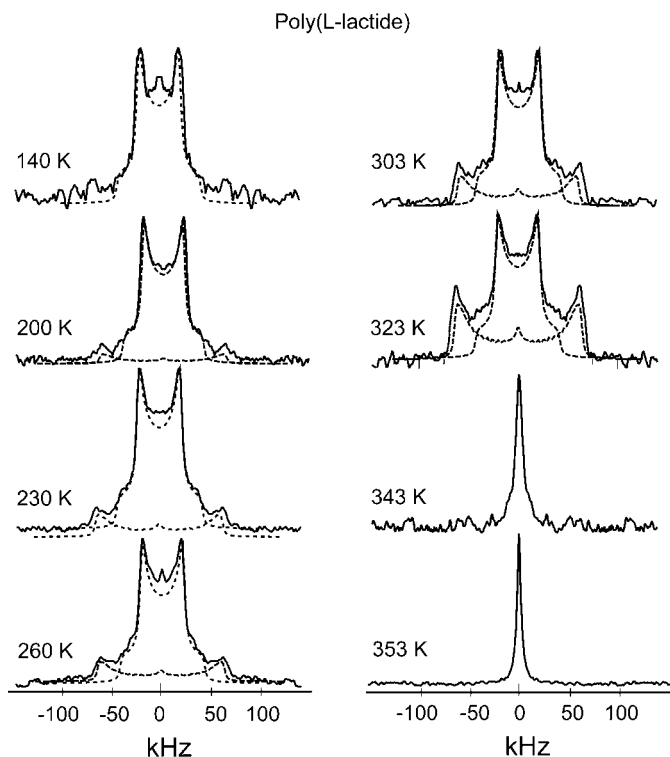


Fig. 6. ^2H NMR line-shape of the selectively deuterated poly(L-lactide) at different temperatures. The simulated ^2H NMR line-shapes for the methyl and terminal hydroxyl groups undergoing the three- and two-fold symmetry reorientations, respectively, are superimposed in the spectra, as shown by the dashed lines.

between nuclei within a molecule, is dependent on the molecular structure according to the equation [38]

$$M_2^{\text{intra}} = 358.082N_0^{-1} \sum_i n_i \sum_{i \neq j} r^{-6}, \quad (1)$$

where N_0 is the number of protons in a molecule, n_i is the number of structurally equivalent protons of type i per molecule, and r is the distance between the i th and j th protons in Å units. The intramolecular contributions were calculated using the positions of protons through minimizing the potential energy of the molecule with the Gaussian program [39]. In our calculations, two different motional states in the molecule were considered: the reorientation of the methyl groups around their three-fold symmetry (C_3) and the reorientation of the hydroxyl groups around their two-fold symmetry (C_2). For the rigid molecule, the calculated M_2 value was 0.158 mT^2 . When the methyl reorientation was considered, the calculated M_2 value was decreased to 0.107 mT^2 . Furthermore, if the hydroxyl reorientation was taken into account, in addition to the fast methyl reorientation, the value of M_2 obtained was 0.097 mT^2 . The M_2 contribution of the methine protons is believed to be rather small due to the nature of its rigid structure and will be neglected from a further discussion. Table 1 lists the calculated M_2 values of the molecule at different motional states.

Table 1
Calculated and experimental values of the proton second moments of PLLA

Motion	M_2 calculated ($\times 10^{-2} \text{ mT}^2$)	M_2 experimental ($\times 10^{-2} \text{ mT}^2$)
Stationary molecule	15.8	
$\text{CH}_3^{\text{intra}} (C_3)$	10.7	11
$\text{CH}_3^{\text{intra}}-\text{OH} (C_3-C_2)$	9.7	8
$\text{CH}_3^{\text{inter}} (C_3)$	3.1	—
S_2^{inter} (by Smith) [35,36]	2.04	—

The intermolecular contribution to the second moment, due to the interactions between nuclei in neighboring molecules, is given by [38]

$$M_2^{\text{inter}} = 358.1(4\pi N_0 \rho / 3R^3 1.66M), \quad (2)$$

where ρ is the density in g/cm^3 , R is the molecular radius in Å, and M refers to the molecular weight in atomic unit (abbreviated as a.u.). For the PLLA sample studied here, $\rho = 1.276 \text{ g/cm}^3$, $R = 3 \text{ Å}$, and $M = 149 \text{ a.u.}$ Therefore, the calculated M_2 value was 0.031 mT^2 . For comparison, we also used the Smith method [40,41] to calculate the intermolecular contributions, as listed in Table 1.

As shown in Fig. 2, the measured M_2 value was about 0.11 mT^2 at 90 K and $0.08 \pm 0.005 \text{ mT}^2$ in the temperature range of 130–325 K. By comparing the experimental data with the calculated results, we can reasonably conclude that the methyl group reorientation plays a major role at temperatures below 323 K. Based on the theoretical calculations, the contribution of the hydroxyl reorientations to the M_2 value is just about 0.01 mT^2 , which is within the error bars of the measured M_2 values. Therefore, the measured M_2 value is not sensitive to the hydroxyl reorientation taking place in the temperature range of 200–325 K, which is observed in the ^2H spectra as shown in Fig. 6.

4.2. ^1H spin-lattice relaxation times

Since ^1H spin-lattice relaxation in PLLA is entirely governed by proton dipolar interactions modulated by reorientational motions involving a single correlation time, the proton spin-lattice relaxation rate ($1/T_1^{\text{H}}$) can be described by the BPP model [42]:

$$\frac{1}{T_1^{\text{H}}} = C \left(\frac{\tau_c}{1 + \omega_0^2 \tau_c^2} + \frac{4\tau_c}{1 + 4\omega_0^2 \tau_c^2} \right), \quad (3)$$

where τ_c is the correlation time describing the dynamic process, ω_0 is the Larmor angular frequency, and C is a dipole–dipole relaxation constant, which is associated with proton–proton distances and is also proportional to the reduction of the second moment (ΔM_2) induced by the molecular motions according to [43,44]

$$C = \frac{2}{3} \Delta M_2 \gamma_{\text{H}}^2, \quad (4)$$

where γ_{H} is the proton gyromagnetic ratio.

For thermally activated diffusion, the correlation time τ_c is usually described in the Arrhenius form

$$\tau_c = \tau_0 \exp \frac{E_a}{RT}, \quad (5)$$

where τ_0 is the pre-exponential factor corresponding to the rotational correlation time at the infinitive temperature, R is the gas constant, T is the absolute temperature, and E_a stands for the activation energy (per mole) for the dynamic process.

The two sets of the T_1^H data obtained from the bi-exponential recoveries were fitted using Eqs. (3)–(5), as indicated by the solid lines in Fig. 5. Table 2 lists all parameters yielded from the fittings. Obviously, both the amorphous and crystalline phases have about the same activation energy. However, there is a significant difference in C , which implies the difference in the motional states associated with the amorphous and crystalline phases in the biopolymer. For the amorphous phase, the ΔM_2^a value derived from Eq. (4) was 0.105 mT^2 , while the ΔM_2^c value was 0.031 mT^2 for the crystalline phase.

The total reduction of the second moment in the biopolymer with the coexistence of the amorphous and crystalline phases can be rationalized by

$$\Delta M_2^{\text{total}} = p_c \times \Delta M_2^c + p_a \times \Delta M_2^a, \quad (6)$$

where ΔM_2 is the reduction of the second moment due to the motions associated with a specific molecular phase having a fraction of p in the biopolymer, and a and c refer to the crystalline and amorphous phases coexisting in PLLA, respectively. In our preceding discussions, we obtained $\Delta M_2^c = 0.031 \text{ mT}^2$, $\Delta M_2^a = 0.105 \text{ mT}^2$, $p_c = 0.46$, and $p_a = 0.54$ (c.f. Fig. 4). Therefore, the total ΔM_2 calculated based on Eq. (6) was 0.070 mT^2 . It can be calculated from Fig. 2 that from the rigid state at the low temperature to the plateau of 0.080 mT^2 the reduction of the second moment is 0.079 mT^2 . Therefore, the total reduction of the second moment, $\Delta M_2^{\text{total}}$ derived from Eq. (6) is in good agreement with the experimental value (c.f. Fig. 2), after taking into account the M_2 contribution of 0.01 mT^2 due to the hydroxyl reorientations. In other words, the hydroxyl reorientations below T_g play a secondary role in the relaxation mechanism and cannot be characterized by the proton relaxations.

Table 2
Motional parameters obtained from the ^1H relaxation measurements

	^1H relaxation parameters	
	Amorphous phase	Crystalline phase
C ($\times 10^9 \text{ S}^{-2}$)	5.0	1.5
E_a (kJ/mol)	7.8	7.3
τ_0 ($\times 10^{-12} \text{ s}$)	2.4	2.9

4.3. ^2H spin-lattice relaxation times

Nuclei with spin of $I \geq 1$ possess an electrical quadrupole moment eQ which interacts with the electrical field gradient (EFG). Fluctuation of the EFG is a major relaxation mechanism in the case of quadrupolar nuclei. Similarly, the ^2H spin-lattice relaxation rate ($1/T_1^D$) can be also described by the BPP model [45,46]:

$$\frac{1}{T_1^D} = \frac{3}{50} \pi^2 \left[\frac{2I+3}{I^2(2I-1)} \right] \chi^2 \left(\frac{\tau_c}{1+\omega_0^2\tau_c^2} + \frac{4\tau_c}{1+4\omega_0^2\tau_c^2} \right), \quad (7)$$

where τ_c is the correlation time describing the dynamic process, ω_0 is the Larmor angular frequency, and χ is the quadrupole coupling constant given by e^2qQ/h . Similar to ^1H , the correlation time τ_c can be described in the same Arrhenius form as in Eq. (5).

All of the ^2H experimental data obtained from the relaxation measurements were fitted using Eqs. (5) and (7) as indicated by the solid lines in Fig. 5, yielding $E_a = 6.5 \text{ kJ/mol}$ and $\tau_0 = 1.7 \times 10^{-12} \text{ s}$. The activation energy obtained here is very similar to that of other biopolymers having methyl and hydroxyl functional groups [47], such as polyhydroxypropyl methyl cellulose, polymethyl cellulose, and polyhydroxypropyl cellulose. It can also be noticed from Fig. 5 that there exists a different T_1^D relaxation behavior when the temperature is above T_g (i.e. $\beta = 3.09 \text{ K}^{-1}$), as indicated by the vertical line.

4.4. ^2H NMR lineshapes

It is well known [27,28,48–50] that the quadrupolar splitting of the ^2H spectrum of a single crystal placed in an external magnetic field B_0 can be described by

$$\nu = \nu_0 \pm \frac{3}{8} \chi (3 \cos^2 \theta - 1 - \eta \sin^2 \theta \cos 2\varphi), \quad (8)$$

where ν_0 is the ^2H Larmor frequency, χ is the quadrupole coupling constant given by e^2qQ/h , and η is the asymmetry parameter of the EFG tensor. The angles θ and φ describe the orientation of the \mathbf{B}_0 in the principal axis system of the quadrupole coupling tensor.

For polycrystalline as well as for the rigid amorphous samples, all orientations of a C–D bond are equally distributed and the spectrum becomes the so-called Pake-doublet [51,52]. For aliphatic deuterons, the EFG tensor is more or less cylindrically symmetric about C–D and asymmetry parameter is close to zero. Thus, in the absence of molecular motion, the splitting $\Delta\nu$ between the singularities of the Pake-doublet is $3/4\chi$, [53] where χ is the static quadrupolar coupling constant.

Typically, the reorientation of the C–D bond reduces the EFG and thus results in a change of the line-shape, depending on the nature and frequency of the motional processes involved. If the rate of the molecular motion is greater than the quadrupolar-coupling constant, the

spectral splitting $\Delta\nu$ becomes [54]

$$\Delta\nu = \frac{3}{4} \chi (3 \cos^2 \theta_{C-D} - 1), \quad (9)$$

where θ_{C-D} describes the orientation of the C–D vector with respect to the motional axis and the brackets represent the spatial averaging over all orientations.

It is seen clearly from Fig. 6 that the two Pake-doublets with quadrupolar splittings of 37 and 116 kHz are superimposed. This implies that the two different deuterons in the PLLA (i.e. the methyl and hydroxyl groups as indicated in Scheme 1) are distinguishable. Fig. 7 shows the possible reorientation for the methyl three-fold reorientation (C_3) and for the hydroxyl two-fold reorientations (C_2) in the PLLA. With the tetrahedral geometry of the CD_3 group, the orientation of the C–D bond with respect to the CD_3 rotational axis is 70.5° (i.e. $\theta_{C-D} = 70.5^\circ$). For the hydroxyl group, the O–D vector is flipped along the C–O bond (i.e. $\theta_{O-D} = 78^\circ$). Thus 2H NMR spectra can be simulated by using the cone model as described by Macho et al. [55,56]. For the methyl group, the three equally populated equilibrium positions (at the jump rate of $1 \times 10^7 s^{-1}$) with $\theta_{C-D} = 70.5^\circ$, $\phi = 120^\circ$, and $\chi = 128$ kHz were used in our simulations. While for the hydroxyl group, the two equally populated positions (at the jump rate of $1 \times 10^6 s^{-1}$) with $\theta_{O-D} = 78^\circ$, $\phi = 180^\circ$, $\chi = 136$ kHz were used. The simulated spectra are shown by the dashed lines in Fig. 6. It is worth noting that the 2H spectra could be axially asymmetric for the two-fold flip as in the case of hydroxyl group. However, the hydroxyl 2H spectra observed here appear to be axially symmetric. This may be

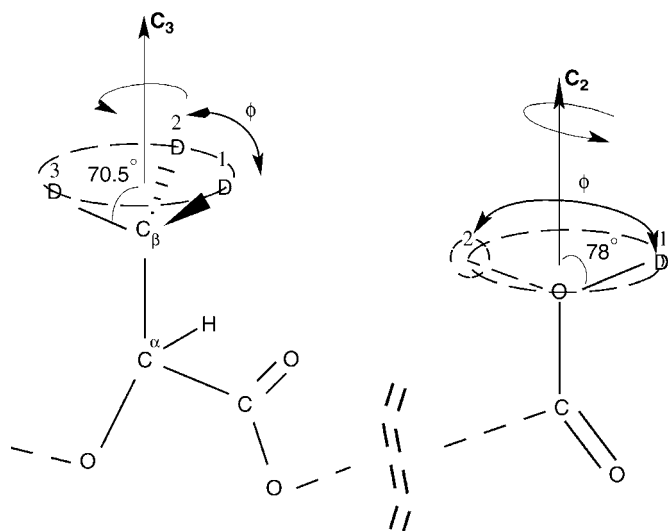


Fig. 7. Model of the PLLA structure for the methyl three-fold reorientation (C_3) and the terminal hydroxyl two-fold reorientation (C_2). The reorientational axes are the C^α – C^β and C–O bonds for the methyl and hydroxyl groups, respectively. For the simulation of 2H spectra, the three equally populated equilibrium positions of the CD_3 group with $\theta_{O-D} = 70.5^\circ$, $\phi = 120^\circ$ and $\chi = 128$ kHz were used for the methyl groups, while the two equally populated positions (with the jump rate of $1 \times 10^6 s^{-1}$) of the hydroxyl group with $\theta_{O-D} = 78^\circ$, $\phi = 180^\circ$, $\eta = 0$ and $\chi = 136$ kHz were used for the hydroxyl groups.

the result of the rapid reorientation of the O–D termini which motionally scales the EFG tensor, as in the case of polyhydroxybutyric acid (PHB) [17]. In the case of PLLA, the quadrupolar coupling constant obtained from the fitting is just 136 kHz for the O–D termini, which is much smaller than ~ 240 kHz obtained in the rigid water [57]. In addition, the fluctuation of molecular axis might further reduce the QCC values and spectral intensities [58]. In fact, even in the case of rigid water with a very large quadrupolar coupling constant (e.g. ~ 240 kHz), nearly axially symmetric spectra were observed.

At very low temperature (e.g. 140 K), the two-fold reorientation of the O–D termini might be rather slow that the EFG tensor could not effectively attenuated by the reorientation. Thus, the resulting 2H spectrum becomes very broad due to the large quadrupolar interaction, so that it could hardly be observed with a relatively long $\pi/2$ pulse length (i.e. $3 \mu s$) used in our experiments. Therefore, the 2H spectrum shows only the methyl group with a quadrupolar splitting of 37 kHz. The fast reorientation of the O–D termini starts at ~ 200 K resulting in an additional Pake-doublet with a quadrupolar splitting of 116 kHz, as shown in Fig. 6. When the temperature increase further, more and more termini hydroxyl groups in the segments of the biopolymer chains are involved in the fast hydroxyl reorientation, resulting in the increase of the intensity stemming from the motional hydroxyl groups, although its integral intensity is much smaller than that of the methyl group. Therefore, there exist not only the methyl reorientations but also the termini hydroxyl reorientations in the temperature range of 200–323 K, which corroborates the results obtained from the 1H M_2 measurements. When the temperature goes above T_g (i.e. 323 K), the segments of the biopolymer chains start to break down or the so-called onset of the entangled process [59], and eventually reaches a liquid state upon the melting of the biopolymer. Consequently, a single narrow 2H NMR peak was observed at temperatures higher than 330 K, as shown in Fig. 6. This process is in fact reflected in the plot of the proton second moment versus temperature, as shown in Fig. 2, where the 1H M_2 decreases further as the temperature goes above T_g (i.e. 323 K) and reaches the second plateau of $0.03 mT^2$ at T_m (i.e. 448 K).

It is worth noting that the activation energy and relaxation times (i.e. the molecular dynamics) of biopolymers with a molecular weight between 1000 and 50,000 g/mol, to some extent, are almost independent of the molecular weight [17]. Therefore, we can globally discuss the molecular dynamics of the PLLA ($M_w = 20,000$ g/mol) and that of deuterated PLLA ($M_w = 8,600$ g/mol).

5. Conclusion

The molecular dynamics of the PLLA biopolymer has been well characterized by various wide-line 1H and 2H solid-state NMR techniques. Our results indicate that the methyl groups' three-fold (C_3) reorientation and the

hydroxyl groups' two-fold (C_2) reorientation are the two major motions existing in the polymer. For instance, the methyl group rotation is dominant at low temperature (e.g. 90 K), while the hydroxyl reorientation plays an important role in the dynamics when the temperature is above the glass transition temperature T_g of 323 K. In the temperature range of 200–325 K, both the methyl and hydroxyl reorientations coexist in PLLA, although the former plays a much greater role in the dynamics than the latter one. In other words, our results imply that the backbone chain is relatively rigid, up until the melting of the biopolymer.

It has also been demonstrated here that the combined use of various NMR techniques is a powerful approach to study the molecular dynamics. The proton second moment M_2 reflects the molecular motions that reduce the proton dipolar interaction. For instance, the significant M_2 reductions occur at temperatures below 130 K, where the motion of the methyl groups reduces the ^1H – ^1H dipolar interaction in PLLA, and at about 330 K, at which the segment of the polymer chains starts to break down, eventually the chains entangled process starts. However, the measured M_2 value is much less sensitive to the additional hydroxyl reorientation taking place in the temperature range of 200–325 K. However, the hydroxyl reorientation is clearly illustrated by the ^2H NMR line-shapes. Furthermore, in combination with the ^2H spin-lattice relaxation measurements, the ^2H NMR line-shape analyses of the Pake-doublets yield the detailed motional models for the methyl and hydroxyl groups. While the ^1H spin-lattice relaxation allows us to differentiate the amorphous and crystalline phases in the PLLA biopolymer and their respective motional reductions of the ^1H M_2 values, which cannot be achieved from the proton M_2 measurements. However, it cannot reflect the hydroxyl reorientations existing in PLLA. Therefore, the combination of various NMR techniques has great utility in characterizing the molecular dynamics of polymers.

Acknowledgement

We wish to thank Dr. Jean-Louis Morgat for providing the selectively deuterated PLLA sample. This work was supported by the In-House Research Program at the National High Magnetic Field Laboratory supported by National Science Foundation Cooperative Agreement DMR-0084173 and the State of Florida, and in part by the Department of Macromolecular Physics, Adam Mickiewicz University of Poznan, Poland.

References

- [1] E.P. Goldberg, A. Nakajima, *Biomedical Polymers: Polymeric Materials and Pharmaceuticals for Biomedical Use*, Academic Press, New York, 1980.
- [2] C.G. Gebelein, F.K. Koblitz, *Biomedical and Dental Applications of Polymers*, Plenum Press, New York, 1981.
- [3] E. Chiellini, P. Giusti, *Polymers in Medicine: Biomedical and Pharmacological Applications*, Plenum Press, New York, 1983.
- [4] S.W. Shalaby, *Polymers as biomaterials*, Plenum Press, New York, 1984.
- [5] J. Kahovec, B. Sedláček, *Polymers in medicine and biology: short special lectures and posters presented at the 26th Microsymposium on Macromolecules: in Prague, Czechoslovakia, July 1984*, Huethig & Wepf, Basel, New York, 1985.
- [6] M. Rosoff, *Controlled Release of Drugs: Polymers and Aggregate Systems*, VCH Publishers, New York, NY, 1989.
- [7] E. Dickinson, *Food Polymers, Gels and Colloids*, Royal Society of Chemistry, Cambridge, 1991.
- [8] J.W. Boretos, *Concise Guide to Biomedical Polymers; Their Design, Fabrication, and Molding*, Thomas, Springfield, 1973.
- [9] A. Rembaum, M.C. Shen, *Biomed. Polym.* (1971).
- [10] Y.H. Na, Y. He, X. Shuai, et al., *Biomacromolecules* 3 (2002) 1179.
- [11] R.A. Auras, B. Harte, S. Selke, et al., *J. Plast Film Sheeting* 19 (2003) 123.
- [12] T. Miyata, T. Masuko, *Polymer* 38 (1997) 4003.
- [13] T. Miyata, T. Masuko, *Polymer* 39 (1998) 4003.
- [14] P. De Santis, J. Kovacs, *Biopolymers* 6 (1968) 299.
- [15] C. Aleman, B. Lotz, J. Puiggali, *Macromolecules* 34 (2001) 4795.
- [16] F. Nozirov, Z. Fojud, J. Klinowski, et al., *Solid State Nucl. Magn. Reson.* 21 (2002) 197.
- [17] F. Nozirov, Z. Fojud, E. Szczesniak, et al., *Appl. Magn. Reson.* 18 (2000) 37.
- [18] F. Nozirov, M. Kozak, L. Domka, et al., *Mol. Phys. Rep.* 33 (2002) 102.
- [19] F. Nozirov, E. Szczesniak, Z. Fojud, et al., *Solid State Nucl. Magn. Reson.* 22 (2002) 19.
- [20] S. Sosnowski, *Polymer* 42 (2001) 637.
- [21] W. Hoogsteen, A.R. Postema, A.J. Pennings, et al., *Macromolecules* 23 (1990) 634.
- [22] K.A.M. Thakur, R.T. Kean, E.S. Hall, et al., *Macromolecules* 30 (1997) 2422.
- [23] K.A.M. Thakur, R.T. Kean, J.M. Zupfer, et al., *Macromolecules* 29 (1996) 8844.
- [24] R. Freeman, *A Handbook of Nuclear Magnetic Resonance*, Longman Scientific & Technical, Wiley, Harlow, Essex, England, New York, 1987.
- [25] F.A. Bovey, P.A. Mirau, *NMR of Polymers*, Academic Press, San Diego, 1996.
- [26] E.R. Andrew, *Nuclear Magnetic Resonance*, Cambridge University Press, Cambridge, 1969.
- [27] J. Seelig, *Q. Rev. Biophys.* 10 (1977) 353.
- [28] A. Abragam, *The Principles of Nuclear Magnetism*, Clarendon press and Oxford University Press, Oxford, New York, 1983.
- [29] J.H. Davis, K.R. Jeffrey, M. Bloom, et al., *Chem. Phys. Lett.* 42 (1976) 390.
- [30] T. Prellberg, A.L. Owczarek, *Comput. Phys. Commun.* 147 (2002) 629.
- [31] H. Tsuji, in: Y. Doi, A. Steinbuechel, (Eds.), Vol. 4. Wiley-VCH, Weinheim, Germany, 2002, p. 129.
- [32] J. Huang, M.S. Lisowski, J. Runt, et al., *Macromolecules* 31 (1998) 2593.
- [33] I. Dos Santos, J.L. Morgat, M. Vert, *J. Label. Compd. Radiopharm.* 41 (1998) 1005.
- [34] I. Dos Santos, J.L. Morgat, M. Vert, *J. Label. Compd. Radiopharm.* 42 (1999) 1093.
- [35] I. Dos Santos, J.L. Morgat, M. Vert, *Polym. Inter.* 48 (1999) 283.
- [36] K.W. Lee, C.E. Lee, J.Y. Choi, et al., *Solid State Commun.* 133 (2005) 83.
- [37] R. Goc, *Solid State Nucl. Magn. Reson.* 13 (1998) 55.
- [38] J.H. van Vleck, *Phys. Rev.* 74 (1948) 1168.
- [39] M. J. T. Frisch, G. W. Schlegel, H. B. Scuseria, G. E., et al., 1998.
- [40] G.W. Smith, *J. Chem. Phys.* 43 (1965) 4325.
- [41] G.W. Smith, *J. Chem. Phys.* 42 (1965) 4229.
- [42] N. Bloembergen, E.M. Purcell, R.V. Pound, *Phys. Rev.* 73 (1948) 679.

- [43] L. Latanowicz, E.C. Reynhardt, R. Utrecht, et al., *Ber. Bunsenges. Phys. Chem. Chem. Phys.* 99 (1995) 152.
- [44] E.C. Reynhardt, L. Latanowicz, *Chem. Phys. Lett.* 251 (1996) 235.
- [45] G.H. Penner, B.Y. Zhao, K.R. Jeffrey, *Z. Nat. Sec. A* 50 (1995) 81.
- [46] T.W.N. Bieze, J.R.C. Vandermaarel, C.D. Eisenbach, et al., *Macromolecules* 27 (1994) 1355.
- [47] A. Rachocki, J. Tritt-Goc, N. Pis'lewski, *Solid State Nucl. Mag. Reson.* 25 (2004) 42.
- [48] N.J. Salisbury, A. Darke, D. Chapman, *Chem. Phys. Lipids* 8 (1972) 142.
- [49] G. Soda, T. Chiba, *J. Chem. Phys.* 50 (1969) 439.
- [50] A.A. Nevzorov, S. Moltke, M.P. Heyn, et al., *J. Am. Chem. Soc.* 121 (1999) 7636.
- [51] G.E. Pake, *J. Chem. Phys.* 16 (1948) 327.
- [52] G.E. Pake, E.M. Purcell, *Phys. Rev.* 74 (1948) 1184.
- [53] L.J. Burnett, B.M. Muller, *J. Chem. Phys.* 55 (1971) 5829.
- [54] J.C. Rowell, W.D. Phillips, L.R. Melby, et al., *J. Chem. Phys.* 43 (1965) 3442.
- [55] V. Macho, L. Brombacher, H.W. Spiess, *Appl. Magn. Reson.* 20 (2001) 405.
- [56] S. Jurga, V. Macho, B. Hüser, et al., *Z. Phys. B* 84 (1991) 43.
- [57] A.J. Benesi, M.W. Grutzeck, B. O'Hare, et al., *J. Phys. Chem. B* 108 (2004) 17783.
- [58] R.J. Wittebort, E.T. Olejniczak, R.G. Griffin, *J. Chem. Phys.* 86 (1987) 5411.
- [59] N. Fatkullin, R. Kimmich, *J. Chem. Phys.* 101 (1994) 822.